Engineering with Computers
https://doi.org/10.1007/s00366-020-01085-w

ORIGINAL ARTICLE

Stochastic fractal search-tuned ANFIS model to predict blast-induced air overpressure

Jinbi Ye[1] · Juhriyansyah Dalle[2] · Ramin Nezami[3] · Mahdi Hasanipanah[4] · Danial Jahed Armaghani[5]

Received: 23 April 2020 / Accepted: 3 June 2020

Abstract
Air overpressure (AOp) induced by rock blasting is an undesirable phenomenon in open-pit mines and civil construction works. The prediction of AOp has been always a complicated task since many parameters have potential to affect the propagation of air waves. This study aims to assess the capability of a new hybrid evolutionary model based on an integrated adaptive neuro-fuzzy inference system (ANFIS) with a stochastic fractal search (SFS) algorithm. To assess the reliability and acceptability of ANFIS-SFS model, the particle swarm optimization (PSO) and genetic algorithm (GA) were also combined with ANFIS. The proposed models were developed using a comprehensive database including 62 sets of data collected from four granite quarry sites in Malaysia. Performances of the ANFIS-SFS, ANFIS-GA, and ANFIS-PSO models were checked using statistical functions as the performance criteria. The obtained results showed that the proposed ANFIS-SFS model, with root mean square error of 1.223 dB, provided much higher generalization capacity than the ANFIS-PSO (RMSE of 1.939 dB), ANFIS-GA (RMSE of 2.418 dB), and ANFIS (RMSE of 3.403 dB) models in terms of predicting AOp. This clearly demonstrates the effectiveness of SFS to provide a more accurate model in the AOp prediction field.

Keywords Blasting · Air overpressure · ANFIS · Optimization algorithms

1 Introduction

In recent decades, the number of surface mining operations has dramatically grown across the world. In these operations, the widely used methods of drilling and blasting are of the lowest expense. With every explosion, a huge volume of energy is released in the form of temperature and pressure. Only a small part of the energy released is applied to fragmenting and displacing the rock mass. The rest of the energy causes adverse effects such as air blast, blast vibrations, flyrock, dust, and noise [1–12]. Once blast takes place, explosion-induced gases are suddenly released to atmosphere, which produces air pressure waves. The unspent volume of energy that still exists in these gases elevates the air pressure level exceeding the normal atmospheric level. This phenomenon is recognized as air overpressure (AOp). The AOp can be created due to many reasons, including the gases released into the air after detonation, the rock face displacement, ground vibrations, stemming blowout, and displacement that occurs around the bore hole. In case of any certain block, a different combination of the above issues may form [13].

The air pressure wave propagation has been described as a function of distance; it has been standardized using the cube root of the charge mass [14, 15]. Generally, AOp is an atmospheric pressure wave that contains audible sound with high frequency in addition to sub-audible sound with low frequency that is too low to be heard by human beings. In case there is a sufficient amount of sound pressure, the sound waves may lead to damage. AOp does not result in

✉ Jinbi Ye
yejinbi@xmut.edu.cn

✉ Mahdi Hasanipanah
Hasanipanahmahdi@duytan.edu.vn

1 School of Civil Engineering and Architecture, Xiamen University of Technology, Xiamen 361024, Fujian Province, China

2 Department of Information Technology, Universitas Lambung Mangkurat, Banjarmasin 70123, Indonesia

3 Department of Civil Engineering, Faculty of Engineering, Bushehr Branch, Islamic Azad University, Bushehr, Iran

4 Institute of Research and Development, Duy Tan University, Da Nang 550000, Vietnam

5 Department of Civil Engineering, Faculty of Engineering, University of Malaya, 50603 Kuala Lumpur, Malaysia

Published online: 10 June 2020

damage, but causes annoyance; it might lead to a conflict between the managers of the mine and people living in the neighboring area [15, 16].

It is possible to design blasts in a way to keep vibrations and AOp levels in an acceptable limit [15, 17]. Once the waves pass from a certain point, the air pressure rapidly rises; then, it is fallen slowly; afterward, it returns to the ambient value after some oscillations. In this wave, the maximal excess pressure is recognized as the peak air overpressure, which is normally gauged in decibels (dB) with considering the linear frequency weighting (L). Equation (1) can change AOp to dB.

$$\mathrm{AOp} = 20\log\left(\frac{P}{P_{\mathrm{r}}}\right) \tag{1}$$

where $P_{\mathrm{r}} = 2 \times 10^{-6}$ Pa (pressure of the lowest audible sound) and P is the measured AOp in terms of Pa. It is not easy to predict the maximum level of AOp at a certain location with a high accuracy; the reason is the uncontrollable and unpredictable impacts of predominant atmospheric conditions [15]. The cube root is the most commonly used factor in predicting AOp, which incorporates both the distance from the blast face (D) and the maximum charge per delay (MC). An overview of blast design parameters is also shown in Fig. 1. In this figure, B, S, and T are the burden, spacing, and stemming variables, respectively.

In recent years, practitioners and researchers have applied a variety of artificial intelligence techniques to different mining, civil, and geo-engineering applications [18–39]. Khandelwal and Singh [16] developed an ANN for the purpose of predicting AOp. The results obtained by their developed mode were compared to those of the multivariate regression analysis (MVRA). The comparative study confirmed that ANN outperformed the other predictor in terms of predicting AOp. For AOp prediction, support vector machine (SVM) was also developed by Khandelwal and Kankar [40]. SVM was found as an efficient model to predict the AOp in comparison with the generalized predictor equation, and the results showed the superiority of the SVM to the rival in doing the defined task. In the study conducted by Hajihassani et al. [41], the implementation of a hybrid evolutionary model based on integrated neural network (NN) with particle swarm optimization (PSO) was investigated to estimate AOp. The results obtained using the PSO-NN were compared with those of the empirical formula. Findings confirmed that their proposed model performed efficiently regarding the accurate prediction of AOp. Hasanipanah et al. [42] established some models based on ANN, FS, and ANFIS to predict AOp. According to their results, ANFIS showed better performance than the ANN and FS models. In another study, Hasanipanah et al. [43] developed a practical hybrid model by integrating support vector regression (SVR) with PSO for the aim of the AOp prediction. Their statistical results revealed the superiority of PSO-SVM model over SVM in terms of the accuracy level. Alel et al. [44] suggested the application of multi swarm algorithm (MSO) to predict the AOp value and showed its effectiveness in this field. Recently, Nguyen et al. [45] have offered several types of ANN in estimating the AOp. AminShokravi et al. [46] presented the linear and nonlinear equations for the AOp prediction through PSO. According to their results, the prediction accuracy of the PSO-based models was excellent. In another study, hybridization of the random forest (RF) and ANN models for the purpose of predicting AOp was tested by Nguyen and Bui [47]. They showed that the proposed ANN-RF model produced better results than the RF and ANN models. For the same purpose, Zhou et al. [48] offered a hybrid optimization method based on firefly algorithm (FFA) and fuzzy system (FS). They demonstrated the successful application of FFA-FS as an efficient model for predicting AOp. Nguyen and Bui [49] predicted the AOp value through hybridizing the genetic algorithm (GA) with the boosted smoothing spline. To check the acceptability of the GA-boosted smoothing spline model, several other soft computing models were also implemented. According to their results, the proposed GA-boosted smoothing spline model is useful as an alternative model for the prediction of AOp. In another study, Bui et al. [50] offered several soft computing models such as ANN, k-nearest neighbors, SVM, RF, and boosted regression trees for the prediction of AOp. They used 113 datasets gathered from an open-pit mine in Vietnam. Their results indicated that ANN outperformed the other predictive models in terms of root mean square error (RMSE). For the same purpose, the Cubist, gradient boosting machine, and RF models were investigated by

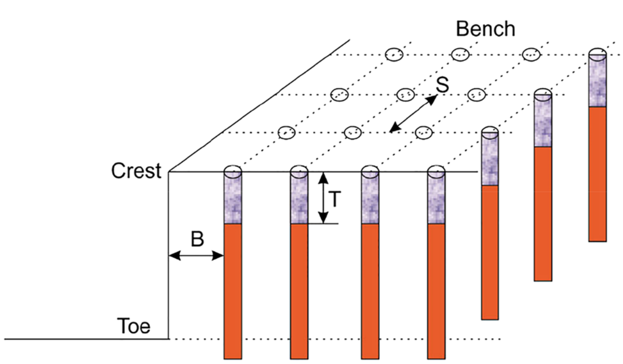

Fig. 1 A view of the blasting pattern structure [50]

Nguyen et al. [51]. They concluded that the lowest RMSE and the highest effectiveness were offered by the Cubist model.

The present study develops a practical hybrid evolutionary model using an integrated adaptive neuro-fuzzy inference system (ANFIS) with a stochastic fractal search (SFS) algorithm aiming at predicting the blast-induced AOp. To assess the reliability and acceptability of the ANFIS-SFS model, two hybrid models of ANFIS optimized with PSO and genetic algorithm (GA) were also used. At the final step, a comparison was made on the predictions made by the models in terms of the accuracy level of the predicted values.

2 Research significance

Study of blasting is especially important to identify the undesirable phenomena, thereby minimizing potential damage to the surroundings. It is well known that the AOp is one of the most particular concerns induced by mine blasting. Therefore, the present study aims to present the accurate and practical models to predict AOp. To this aim, an integrated expert system comprising of ANFIS and SFS algorithm is proposed, and then to check its results, GA and PSO algorithms are also developed. To our knowledge, the ANFIS-SFS model has not been used to predicting the blast-induced AOp in different timescales as of yet.

3 Sources of database

Four quarry sites of granite rock located in Malaysia were taken into consideration, and totally 62 blasting operations were meticulously studied [41]. More specifically, the sites are near the Johor city that is the capital of the Johor State, Malaysia (see Fig. 2). In the sites studied, granite quarry is blasted by means of blast holes of 75, 89, and 115 mm of diameter and the main explosive is ANFO (ammonium

Fig. 2 Sites studied for the prediction of AOp [41]

Table 1 Descriptive statistics for modeling parameters

Parameter	Minimum	Maximum	Mean	Standard error	Standard deviation	Skewness
HD	10	25	15.145	0.495	3.896	0.760
PF	0.34	0.76	0.518	0.014	0.109	−0.027
MC	60	171	88.153	3.422	26.946	1.392
T	1.7	3	2.087	0.034	0.268	1.060
B	1.5	3.2	2.366	0.061	0.483	0.293
S	2.65	4	3.318	0.053	0.421	−0.220
RQD (%)	60	91	76.823	1.222	9.618	−0.174
NoH	12	63	39.871	1.620	12.757	−0.060
D	300	600	498.387	18.179	143.140	−0.699
AOp	89.1	126.3	105.095	1.274	10.034	0.263

HD depth of the blast holes, *PF* powder factor, *MC* maximum charge per delay, *T* stemming, *B* burden, *S* spacing, *RQD* rock quality designation, *NoH* number of holes, *D* distance from the blast point, *AOp* air overpressure

nitrate/fuel oil). The stemming material used in this study is fine gravels. Table 2 describes the blasting sites of the case studies. The parameters taken into account in the data gathering process were *B*, *T*, *S*, powder factor (PF), depth of the blast holes, and rock quality designation (RQD). In each of the blasting operations, AOp was checked by means of VibraZEB instrument. This instrument recorded AOp values that were in the range of 88 dB to 148 dB. In all cases, AOp was measured in front of the quarry bench and roughly perpendicular to it. Remember that *D* ranged from 300 to 600 m in various sites. Descriptive statistics for modeling parameters are shown in Table 1 and Fig. 3. Note that Fig. 3 shows the values of all parameters used in the modeling processes gathered from 62 blasting events. It is worth mentioning that the other parameters such as *B*, *S*, and *T* were determined using blasting design pattern.

4 Predicting the blast-induced AOp

This section describes how SFS, PSO, and GA were implemented to improve the ANFIS performance. The proposed models were first trained using 50 datasets out of 62 datasets (80%); then, they were tested using the rest of datasets (20%).

4.1 Integrated ANFIS with SFS

The ANFIS algorithm, as a popular machine learning method, has been widely used in order to address complex nonlinear problems [52–56]. This efficient algorithm integrates the neural network with the fuzzy inference system [57]. ANFIS makes use of least squares and gradient descent algorithms to perform a learning model [58]. ANFIS has been found a powerful tool applicable effectively to prediction problems. In the following, a five-layer ANFIS is described [58].

Within the first layer, i.e., the fuzzification layer, all nodes are supposed as adaptive inputs.

$$O_i^1 = \mu A_i\left(x_1\right) \quad \text{for } i = 1, 2, \ldots, n \tag{2}$$

$$O_i^1 = \mu B_{i-2}\left(x_2\right) \quad \text{for } i = 3, 4, \ldots, n \tag{3}$$

where $\mu A_i\left(x_1\right)$ and $\mu B_{i-2}\left(x_2\right)$ stand for Gaussian membership functions and n denotes the number of fuzzy sets for different input variables [58].

Within the second layer, i.e., the product layer, every node evaluates the firing strength of specific rule with the use of Eq. 4.

$$O_i^2 = \omega_i = \mu A_i\left(x_1\right)\mu B_i\left(x_2\right) \quad \text{with } i = 1, 2 \tag{4}$$

Within the third layer, i.e., the normalized layer, the normalization process is carried out with the use of Eq. 5 with

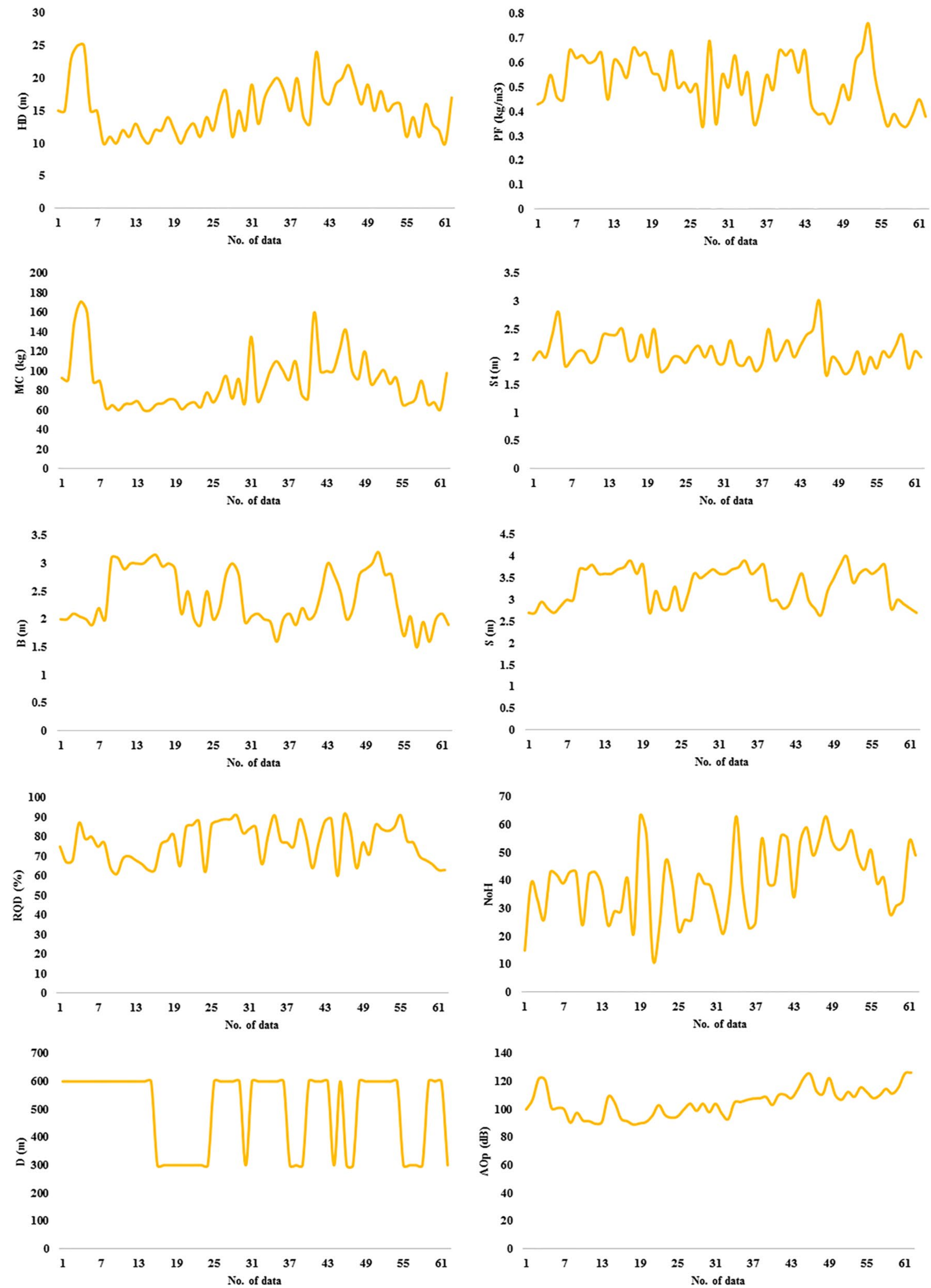

Fig. 3 A view of all parameters used in this study and their values

the summation of the ith rule's firing strength ratio to all rules' firing strength [58].

$$O_i^3 = \bar{w}_i = \frac{w_i}{w_1 + w_2} \quad i = 1, 2 \tag{5}$$

Within the fourth layer, the defuzzification process is carried out. In this layer, each node is adaptable with Eq. 6:

$$O_i^4 = \bar{w}_i f_i = \bar{w}_i \left(k_1^i x + k_2^i y + k_0^i \right) \tag{6}$$

where w_i signifies the output of the third layer and $\left\{k_1^i, k_2^i, k_0^i\right\}$ represents the variable sets of $\bar{w}_i$ node.

Within the fifth layer, i.e., the output layer, the output is formed through summation of the output of the previous layer using Eq. (7):

$$O_i^5 = \text{overall output} = \sum_{\mathrm{i}} \bar{w}_i f_i = \frac{\sum_i w_i f_i}{\sum_i w_i}; \quad i = 1, 2 \tag{7}$$

In ANFIS, three different models are involved, i.e., the fuzzy C-Means clustering (FCM), subtractive clustering (SCM), and grid partitioning (GP). According to the literature that has confirmed FCM as the most effective model, it was chosen for the ANFIS algorithm to be applied to prediction purposes. FCM is elaborated in detail by Nikafshan Rad et al. [57].

In recent years, meta-heuristic algorithms have been successfully implemented when solving a variety of problems, especially for optimization purposes. For instance, SFS is a meta-heuristic algorithm that has been designed based on the natural phenomenon of growth. This algorithm has been found effective in improving ANFIS and optimizing the membership functions elements. More specifically, it is widely known that ANFIS suffers from limitations like quiet convergence and getting trapped in local optima. SFS has the capacity required for enhancing the convergence rate of ANFIS and also helping it to keep distance from local minima. With the use of diffusion, the particles that exist within the new algorithm will be capable of searching the search space with a higher efficiency. Two key parts of optimization in SFS are diffusing and updating processes. During the process of diffusing, each particle diffuses around its current position in a way to satisfy intensification property.

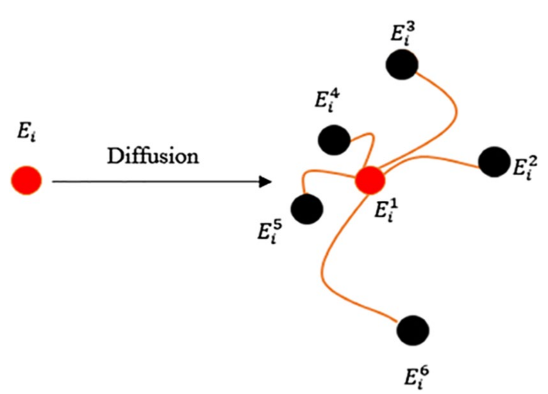

Fig. 4 Particle diffusion [59]

On the other hand, during the process of updating, SFS finds the way each particle in the group can update its own position rather than updating the other particles' position. Based on Fig. 4 [59], the optimal particle created from the diffusing process in SFS is the isolated particle that is admitted; the others are then rejected. In addition, the process of updating gives motivation to researchers to explore properties in meta-heuristic algorithms. At the diffusion step, two statistical techniques exist that can be used for particles production: Levy flight and Gaussian. Early studies have reported faster concentration of the Levy flight in comparison with the Gaussian walk in little generations. However, in exploring global optima, the Gaussian walk is more encouraging [60]. For more detailed information in regard to the SFS algorithm, the study conducted by Salimi [59] can be referred to. The pseudocode of the ANFIS-SFS is presented in Fig. 5.

4.2 ANFIS integrated with PSO and GA

To examine the performance quality of SFS in ANFIS, two popular optimization algorithms, i.e., GA and PSO [61–65], were considered and also applied to the optimization of ANFIS. Additionally, to minimize prediction errors in the present study, a number of parameters were taken into consideration. In the implementation of the models, two techniques were adopted: least square and back-propagation. The optimal number of fuzzy rules was determined using the trial-and-error method.

When modeling GA-ANFIS, the maximum iteration was fixed at 300, and the minimum error was fixed at 1e−5. Moreover, the mutation and crossover rates were set to 0.3 and 0.7, respectively. Furthermore, various values ranging from 50 to 400 were examined in order to reach the optimal number of populations (see Table 2). As can be seen in this table, with fixing the number of populations at 250, the minimum RMSE was obtained. The inertia weight and the

Integrated ANFIS with a SFS

Set the input
Initialize a random population size, No. Rules, No. generations, the maximum diffusion walk (k), the side walk.
While h<Max No. of Iterations **Do**
    Create the population size (particles)
    Calculate the fitness function based on Error function
    For every Particle in the population **Do**
        Call Diffusing Process:
            For j=1 to k **Do**
                A new point will be created: $GW1 = Gussian(\mu_{BP}, \sigma) + (\varepsilon_{XBP} - \varepsilon'_{XPi})$
            End for
        End Call
    End for
End while
    Call Updating Process:
    First Updating Process
    First, all parameters of ANFIS are ranked
    For Every Point of population(P_i), **Do**
        For each component in Population, **Do**
            If rand [0,1]>P_{ai}
                Update the ANFIS parameters
            End If
        End For
    Second Updating Process:
    All points determined by the first updating process are re-ranked
    For Every Point of population(P'_i) of ANFIS parameter, **Do**
        If rand [0,1]>P'_{ai}
            Update the position:
                $P_i^{''} = P_i' - \hat{\varepsilon} \times (P_t' - BP) | \hat{\varepsilon} \leq 0.5$
                $P_i^{''} = P_i' + \hat{\varepsilon} \times (P_t' - P_r') | \hat{\varepsilon} > 0.5$
            End If
        End For
    End For
Train the optimized ANFIS parameters based Stochastic Fractal Optimization
Calculate MSE for ANFIS testing result

Fig. 5 ANFIS-SFS pseudocode

Table 2 Selection of the proper population size in ANFIS-GA

Population size	Network result	
	RMSE	
	Train	Test
50	5.431	5.196
100	4.560	4.239
150	4.672	4.198
200	4.145	3.802
250	3.771	3.039
300	3.819	3.327
350	3.995	3.891
400	4.347	4.105

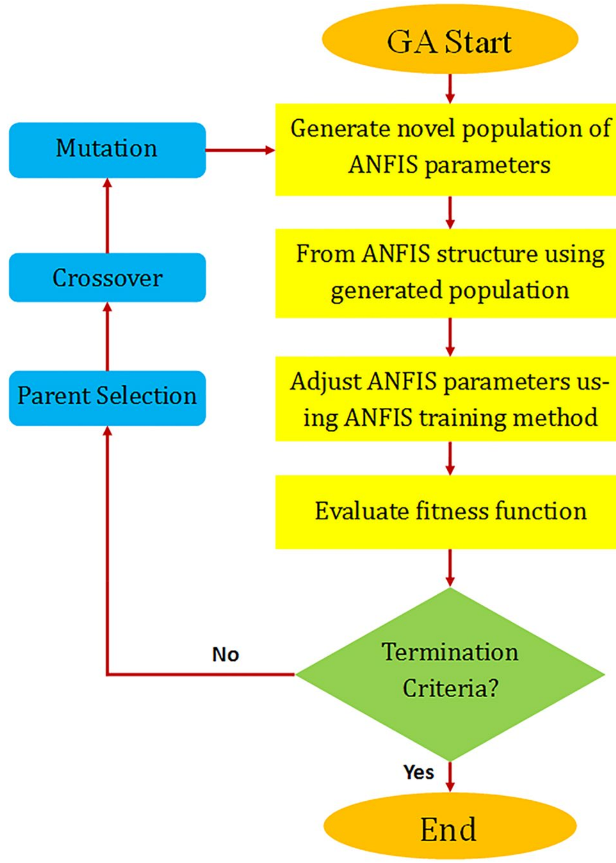

Fig. 6 ANFIS-GA chart [61]

Table 3 Selection of the proper C_1 and C_2 in ANFIS-PSO modeling

C_1	C_2	Network result	
		RMSE	
		Train	Test
1.333	2.667	4.311	3.919
2.667	1.333	4.128	3.877
1.5	1.5	3.722	3.540
2	2	3.295	2.712
1.75	1.75	2.919	2.327
1.5	1.75	3.118	2.774
1.75	1.5	3.541	3.229

Table 4 Selection of the proper number of particles in ANFIS-PSO modeling

No. of particle	Network result	
	RMSE	
	Train	Test
50	4.116	3.882
100	3.866	3.559
150	3.528	3.327
200	3.291	2.580
250	2.887	2.115
300	3.157	2.766
350	3.418	3.382
400	3.701	3.644

number of iterations in ANFIS-PSO were set to 1 and 1000, respectively. Moreover, various values were examined for the aim of choosing the optimal number of particles and coefficients of velocity equation (C_1 and C_2), as shown in Tables 3 and 4. These tables show that the minimum RMSE were attained for $C_1 = C_2 = 1.75$ and the number of particles = 250. As a result, these values were applied to experiments carried out in the present paper. Figures 6 and 7 illustrate the ANFIS schemes optimized using the GA and PSO algorithms.

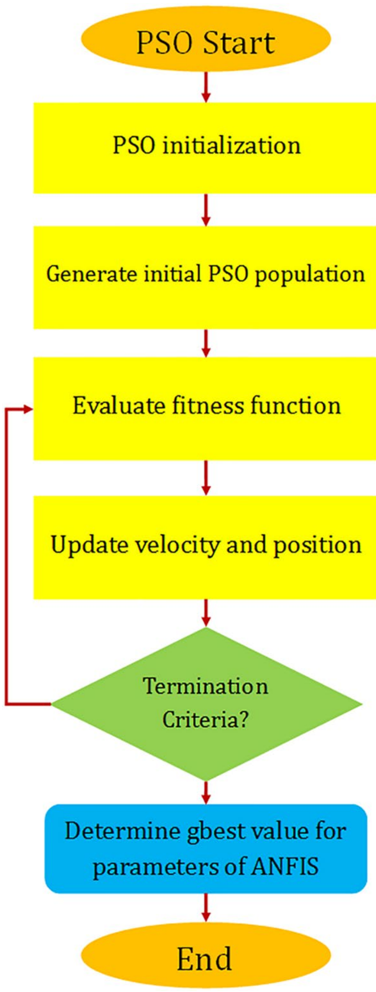

Fig. 7 ANFIS-PSO chart [61]

5 Results and discussion

The present paper was aimed at examining the efficiency of the SFS algorithm in optimizing ANFIS to predict blast-induced AOp. In this section, the way the ANFIS-SFS model performed in regard to the AOp prediction is discussed; after that, the results obtained from the proposed ANFIS-SFS model will be compared to those of the other models. As mentioned earlier, a total of 62 datasets were applied to this study, among which 50 datasets were allocated to training and 12 datasets were allocated to testing purposes. Then, the ANFIS-SFS model performance was assessed regarding RMSE, mean absolute error (MAE), mean average percentage error (MAPE), and coefficient of determination (R^2) [66–80]:

$$\mathrm{MAE} = \frac{1}{n}\sum_{i=1}^{n}\left|A_i - P_i\right| \tag{8}$$

$$\mathrm{RMSE} = \sqrt{\frac{\sum_{i=1}^{n}(A_i - P_i)^2}{n}} \tag{9}$$

$$\mathrm{MAPE} = \left[\frac{1}{n}\sum_{i=1}^{n}\frac{\left|A_i - P_i\right|}{A_m}\right] \times 100 \tag{10}$$

where n stands for the number of data ($n = 62$), and A_i and P_i signify the actual and predicted AOp values, respectively. Table 5 presents the RMSE, MAE, and MAPE (%) values attained by the predictive models. The table shows that the SFS-ANFIS outperformed the others in terms of predicting the AOp value. In addition, Figs. 8, 9, 10, and 11 demonstrate the actual versus estimated AOp values with the use of all predictive models. Accordingly, SFS was found more

Table 5 Assessment of the performance of the prediction models used in this study

Statistical functions	Prediction models							
	ANFIS		ANFIS-GA		ANFIS-PSO		ANFIS-SFS	
	Train	Test	Train	Test	Train	Test	Train	Test
RMSE	4.569	3.403	3.450	2.418	2.817	1.939	1.814	1.223
MAE	4.234	3.242	3.194	2.325	2.626	1.891	1.694	1.133
MAPE (%)	4.112	2.843	3.101	2.039	2.550	1.659	1.645	0.994
R^2	0.904	0.873	0.945	0.935	0.963	0.965	0.987	0.986

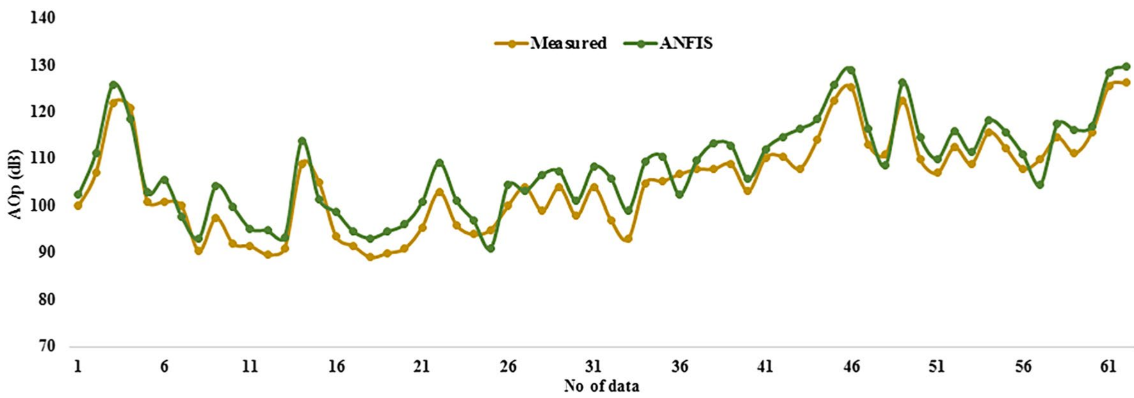

Fig. 8 Use of ANFIS in predicting AOp

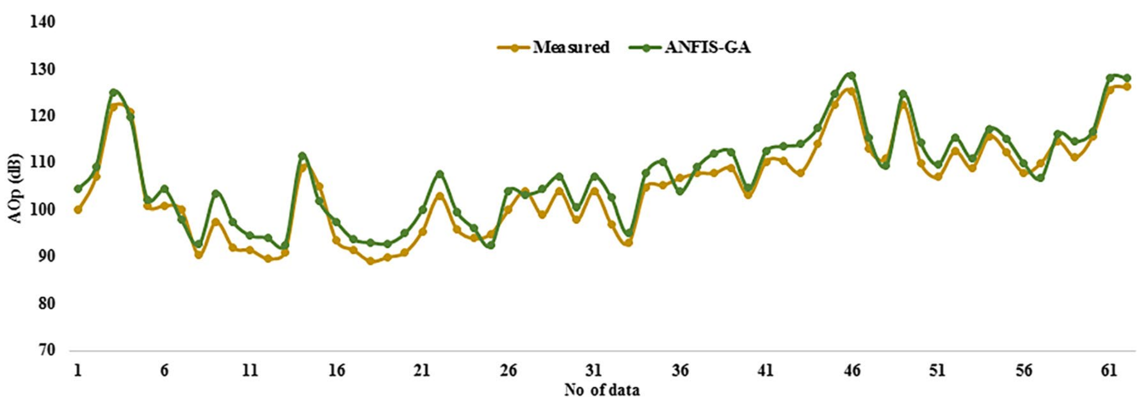

Fig. 9 Use of ANFIS-GA in predicting AOp

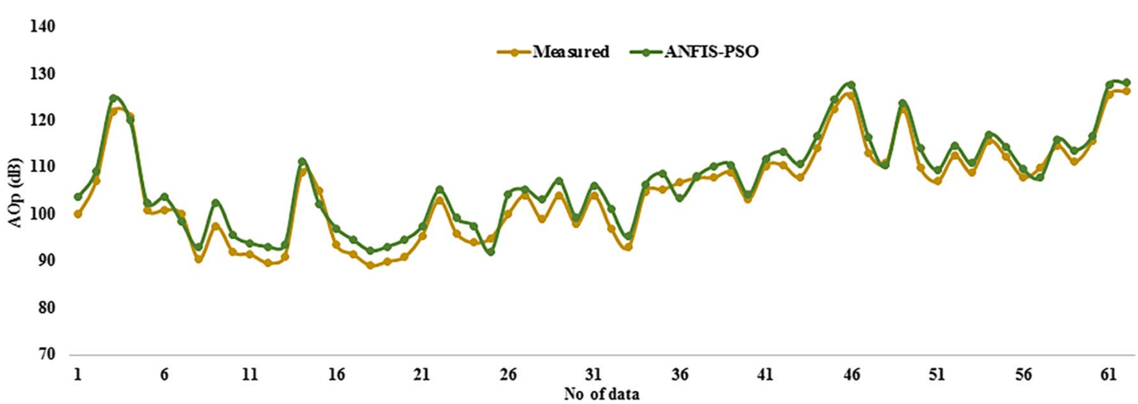

Fig. 10 Use of ANFIS-PSO in predicting AOp

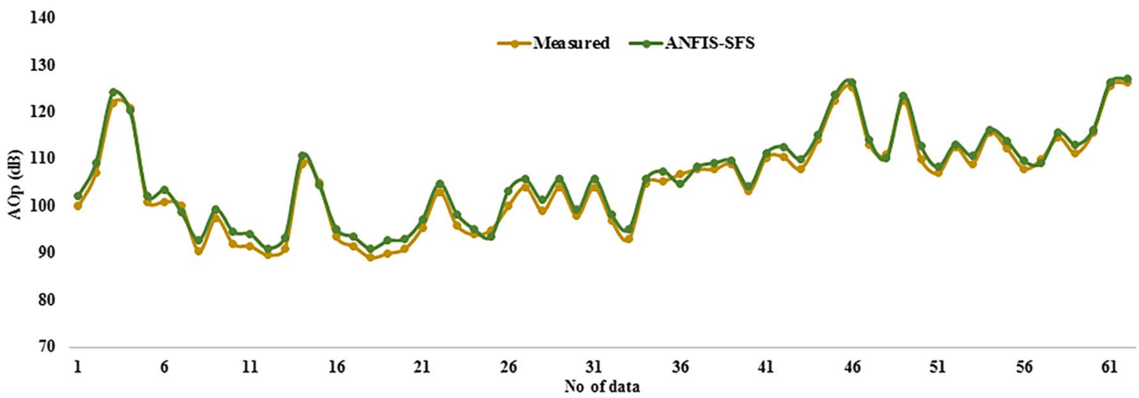

Fig. 11 Use of ANFIS-SFS in predicting AOp

effective in comparison with GA and PSO in regard to the ANFIS improvement. For a better understanding, the Taylor diagrams for both training and testing phases are shown in Fig. 12. Observing Fig. 12, it can be seen that the proposed ANFIS-SFS model was more effective than the others. In addition, the Yang and Zang's [81] method was used to conduct a sensitivity analysis for the aim of showing the relative effect of HD, PF, MC, T, B, S, RQD, NoH, and D upon AOp:

$$r_{ij} = \frac{\sum_{k=1}^{n} \left(y_{ik} \times y_{ok} \right)}{\sqrt{\sum_{k=1}^{n} y_{ik}^2 \sum_{k=1}^{n} y_{ok}^2}} \tag{11}$$

The values of r_{ij} indicate the impact of each input upon the output. With the use of Eq. 10, the values of r_{ij} for HD, PF, MC, T, B, S, RQD, NoH, and D were calculated, as shown in Fig. 13. These results confirmed that T was the most effective parameter upon AOp.

6 Conclusions

Any blasting operation unavoidably leads to different undesirable effects such as air overpressure (AOp). As a result, it is of high importance to predict AOp with a high accuracy in a way to determine properly the safe regions around the operation sites. This paper represents several hybrid evolutionary models based on ANFIS optimized by SFS, PSO, and GA to predict AOp. It is worth mentioning that this is the first work that predicts AOp through ANFIS-SFS model. A database was created containing 62 datasets collected from blasting events performed at four quarry sites in Malaysia [41]. More specifically, the database included 62 sets of data, nine independent parameters, and one dependent parameter. In the predictive models, the independent parameters were set as inputs, and the dependent parameter (AOp) was set as output. Finally, some statistical functions were designed to demonstrate the capacity and superiority of the proposed models in the prediction of AOp. The conclusions of this study are as follows: (1) The use of SFS, GA, and PSO algorithms had a positive impact on the ANFIS

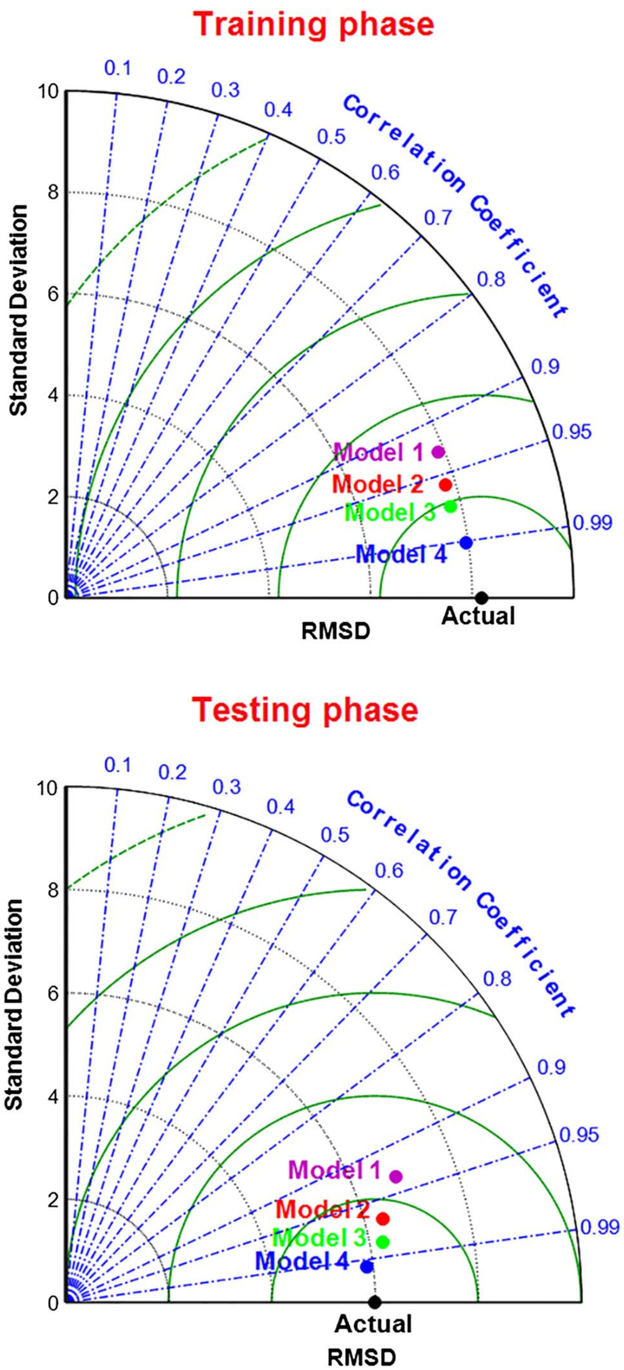

Fig. 12 Obtained Taylor diagrams from model 1: ANFIS, model 2: ANFIS-GA, model 3: ANFIS-PSO, and model 4: ANFIS-SFS for both training and testing phases

performance. (2) The results obtained in this research confirmed that the ANFIS-SFS was the most effective model in regard to accuracy in AOp prediction. In case of ANFIS-SFS, the values of R^2, RMSE, MAE, and MAPE were obtained as 0.986, 1.223, 1.133, and 0.994%, respectively. As a result, SFS could meaningfully enhance the ANFIS performance quality. (3) The ANFIS-SFS model can have the capacity required for addressing other prediction problems that appear generally in the context of rock blasting. (4) Obtained results show that the ANFIS-SFS model can be used with confidence for future research works on predicting the AOp. (5) According to the sensitivity analysis results, the stemming (T) was the most effective parameter on the intensity of AOp. (6) To enhance the ANFIS performance, other meta-heuristic algorithms, including the green heron optimization algorithm, gradient evolution algorithm, firework algorithm, honey bee mating optimization, and interior search algorithm, can be implemented, too.

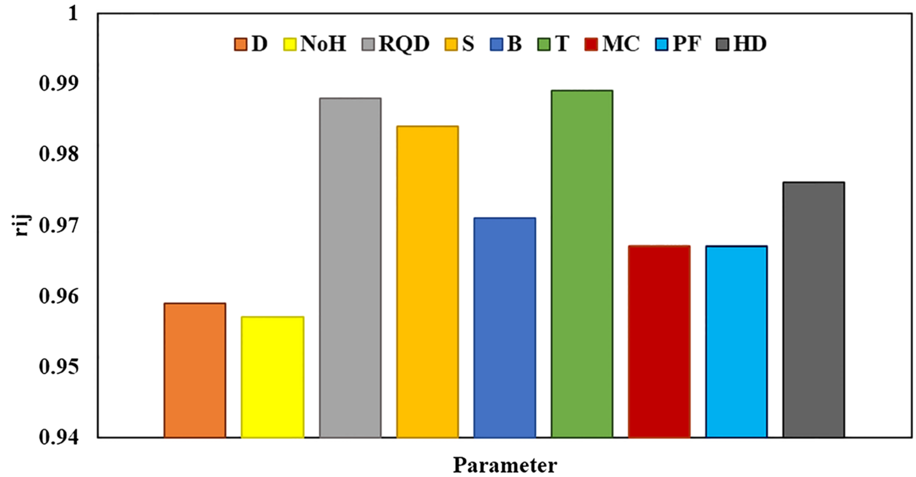

Fig. 13 Results of sensitivity analysis

References

1. Marto A, Hajihassani M, Armaghani DJ, Tonnizam Mohamad E, Makhtar AM (2014) A novel approach for blast induced flyrock prediction based on imperialist competitive algorithm and artificial neural network. Sci World J 5:643715
2. Hajihassani M, Armaghani DJ, Monjezi M, Mohamad ET, Marto A (2015) Blast-induced air and ground vibration prediction: a particle swarm optimization-based artificial neural network approach. Environ Earth Sci 74(4):2799–2817
3. Jahed Armaghani D, Mohamad ET, Hajihassani M, Abad SANK, Marto A, Moghaddam MR (2015) Evaluation and prediction of flyrock resulting from blasting operations using empirical and computational methods. Eng Comput 32(1):109–121
4. Yang H, Hasanipanah M, Tahir MM, Bui DT (2019) Intelligent prediction of blasting-induced ground vibration using ANFIS optimized by GA and PSO. Nat Resour Res. https://doi.org/10.1007/s11053-019-09515-3
5. Keshtegar B, Hasanipanah M, Bakhshayeshi I, Sarafraz ME (2019) A novel nonlinear modeling for the prediction of blast-induced airblast using a modified conjugate FR method. Measurement 131:35–41
6. Yang H, Nikafshan Rad H, Hasanipanah M, Amnieh HB, Nekouie A (2019) Prediction of vibration velocity generated in mine blasting using support vector regression improved by optimization algorithms. Nat Resour Res. https://doi.org/10.1007/s11053-019-09597-z
7. Hasanipanah M, Golzar SB, Larki IA, Maryaki MY, Ghahremanians T (2017) Estimation of blast-induced ground vibration through a soft computing framework. Eng Comput 33(4):951–959
8. Hasanipanah M, Naderi R, Kashir J, Noorani SA, Aaq Qaleh AZ (2017) Prediction of blast produced ground vibration using particle swarm optimization. Eng Comput 33(2):173–179
9. Gao W, Karbasi M, Hasanipanah M, Zhang X, Guo J (2018) Developing GPR model for forecasting the rock fragmentation in surface mines. Eng Comput 34(2):339–345
10. Nikafshan Rad H, Hasanipanah M, Rezaei M, Eghlim AL (2019) Developing a least squares support vector machine for estimating the blast-induced flyrock. Eng Comput 34(4):709–717
11. Ding X, Hasanipanah M, Rad HN, Zhou W (2020) Predicting the blast-induced vibration velocity using a bagged support vector regression optimized with firefly algorithm. Eng Comput. https://doi.org/10.1007/s00366-020-00937-9
12. Li G et al (2020) Developing a new computational intelligence approach for approximating the blast-induced ground vibration. Appl Sci 10(2):434
13. Konya CJ, Walter EJ (1990) Surface blast design. Prentice Hall, Englewood Cliffs
14. Persson PA, Holmberg R, Lee J (1993) Rock blasting and explosives engineering. CRC, Boca Raton, pp 375–377
15. Khandelwal M, Singh TN (2006) Prediction of blast induced ground vibrations and frequency in opencast mine-a neural network approach. J Sound Vib 289:711–725
16. Khandelwal M, Singh TN (2005) Prediction of blast induced air overpressure using neural network. Noise Vib Worldw 36(2):7–16
17. Oriad LL (2002) Explosive engineering, construction vibrations and geotechnology. International Society of Explosives Engineers, Cleveland, p 680
18. Monjezi M, Hasanipanah M, Khandelwal M (2013) Evaluation and prediction of blast-induced ground vibration at Shur River Dam, Iran, by artificial neural network. Neural Comput Appl 22(7–8):1637–1643
19. Hasanipanah M, Armaghani DJ, Monjezi M, Shams S (2016) Risk assessment and prediction of rock fragmentation produced by blasting operation: a rock engineering system. Environ Earth Sci 75(9):808
20. Hasanipanah M, Faradonbeh RS, Armaghani DJ, Amnieh HB, Khandelwal M (2017) Development of a precise model for prediction of blast-induced flyrock using regression tree technique. Environ Earth Sci 76(1):27
21. Apostolopoulou M, Armaghani DJ, Bakolas A, Douvika MG, Moropoulou A, Asteris PG (2019) Compressive strength of natural hydraulic lime mortars using soft computing techniques. Procedia Struct Integr 17:914–923
22. Armaghani DJ, Hatzigeorgiou GD, Karamani Ch, Skentou A, Zoumpoulaki I, Asteris PG (2019) Soft computing-based techniques for concrete beams shear strength. Procedia Struct Integr 17:924–933
23. Asteris PG, Apostolopoulou M, Skentou AD, Antonia Moropoulou A (2019) Application of artificial neural networks for the prediction of the compressive strength of cement-based mortars. Comput Concr 24(4):329–345
24. Asteris PG, Armaghani DJ, Hatzigeorgiou Karayannis CG, Pilakoutas K (2019) Predicting the shear strength of reinforced concrete beams using artificial neural networks. Comput Concr 24(5):469–488

25. Asteris PG, Ashrafian A, Rezaie-Balf M (2019) Prediction of the compressive strength of self-compacting concrete using surrogate models. Comput Concr 24(2):137–150
26. Asteris PG, Mokos VG (2019) Concrete compressive strength using artificial neural networks. Neural Comput Appl. https://doi.org/10.1007/s00521-019-04663-2
27. Asteris PG, Moropoulou A, Skentou AD, Apostolopoulou M, Mohebkhah A, Cavaleri L, Rodrigues H, Varum H (2019) Stochastic vulnerability assessment of masonry structures: concepts, modeling and restoration aspects. Appl Sci 9(2):243
28. Asteris PG, Nikoo M (2019) Artificial bee colony-based neural network for the prediction of the fundamental period of infilled frame structures. Neural Comput Appl 31(9):4837–4847
29. Cavaleri L, Asteris PG et al (2019) Prediction of surface treatment effects on the tribological performance of tool steels using artificial neural networks. Appl Sci 9(14):2788
30. Cavaleri L, Chatzarakis GE, Di Trapani F, Douvika MG, Roinos K, Vaxevanidis NM, Asteris PG (2017) Modeling of surface roughness in electro-discharge machining using artificial neural networks. Adv Mater Res 6(2):169–184
31. Chen H, Asteris PG, Armaghani DJ, Gordan B, Pham BT (2019) Assessing dynamic conditions of the retaining wall using two hybrid intelligent models. Appl Sci 9:1042
32. Hajihassani M, Abdullah SS, Asteris PG, Armaghani DJ (2019) A gene expression programming model for predicting tunnel convergence. Appl Sci 9:4650
33. Huang L, Asteris PG, Koopialipoor M, Armaghani DJ, Tahir MM (2019) Invasive weed optimization technique-based ANN to the prediction of rock tensile strength. Appl Sci 9:5372
34. Psyllaki P, Stamatiou K, Iliadis I, Mourlas A, Asteris PG, Vaxevanidis N (2018) Surface treatment of tool steels against galling failure. MATEC Web Conf 188:04024
35. Sarir P, Chen J, Asteris PG, Armaghani DJ, Tahir MM (2019) Developing GEP tree-based, neuro-swarm, and whale optimization models for evaluation of bearing capacity of concrete-filled steel tube columns. Eng Comput. https://doi.org/10.1007/s00366-019-00808-y
36. Xu H, Zhou J, Asteris PG, Armaghani DJ, Tahir MM (2019) Supervised machine learning techniques to the prediction of tunnel boring machine penetration rate. Appl Sci 9(18):3715
37. Farsa EZ, Ahmadi A, Maleki MA, Gholami M, Rad HN (2019) A low-cost high-speed neuromorphic hardware based on spiking neural network. IEEE Trans Circuits Syst II Express Briefs 66(9):1582–1586
38. Hajihassani M, Kalatehjari R, Marto A et al (2020) 3D prediction of tunneling-induced ground movements based on a hybrid ANN and empirical methods. Eng Comput 36:251–269
39. Hasanipanah M, Amnieh HB (2020) Developing a new uncertain rule-based fuzzy approach for evaluating the blast-induced backbreak. Eng Comput. https://doi.org/10.1007/s00366-019-00919-6
40. Khandelwal M, Kankar P (2011) Prediction of blast-induced air overpressure using support vector machine. Arab J Geosci 4(3–4):427–433
41. Hajihassani M, Jahed Armaghani D, Sohaei H, Tonnizam Mohamad E, Marto A (2014) Prediction of airblast-overpressure induced by blasting using a hybrid artificial neural network and particle swarm optimization. Appl Acoust 80:57–67
42. Hasanipanah M, Armaghani DJ, Khamesi H, Amnieh HB, Ghoraba S (2016) Several non-linear models in estimating air-overpressure resulting from mine blasting. Eng Comput 32(3):441–455
43. Hasanipanah M, Shahnazar A, Amnieh HB, Armaghani DJ (2017) Prediction of air-overpressure caused by mine blasting using a new hybrid PSO–SVR model. Eng Comput 33(1):23–31
44. Alel MNA, Upom MRA, Abdullah RA, Abidin MHZ (2018) Optimizing blastings air overpressure prediction model using swarm intelligence. J Phys Conf Ser 995:012046
45. Nguyen H, Bui XN, Bui HB, Mai NL (2018) A comparative study of artificial neural networks in predicting blast-induced air-blast overpressure at Deo Nai open-pit coal mine, Vietnam. Neural Comput Appl. https://doi.org/10.1007/s00521-018-3717-5
46. AminShokravi A, Eskandar H, Derakhsh AM et al (2018) The potential application of particle swarm optimization algorithm for forecasting the air-overpressure induced by mine blasting. Eng Comput 34:277–285
47. Nguyen H, Bui XN (2019) Predicting blast-induced air overpressure: a robust artificial intelligence system based on artificial neural networks and random forest. Nat Resour Res 28(3):893–907
48. Zhou J, Nekouie A, Arslan CA, Pham BT, Hasanipanah M (2019) Novel approach for forecasting the blast induced AOp using a hybrid fuzzy system and firefly algorithm. Eng Comput. https://doi.org/10.1007/s00366-019-00725-0
49. Nguyen H, Bui XN (2020) Soft computing models for predicting blast-induced air over-pressure: a novel artificial intelligence approach. Appl Soft Comput 92:106292
50. Bui XN, Nguyen H, Le HA, Bui HB, Do NH (2020) Prediction of blast-induced air over-pressure in open-pit mine: assessment of different artificial intelligence techniques. Nat Resour Res 29(2):571–591
51. Nguyen H, Bui X, Tran Q et al (2020) A comparative study of empirical and ensemble machine learning algorithms in predicting air over-pressure in open-pit coal mine. Acta Geophys 68:325–336
52. Hasanipanah M, Shahnazar A, Arab H, Golzar SB, Amiri M (2017) Developing a new hybrid-AI model to predict blast induced backbreak. Eng Comput 33(3):349–359
53. Jiang W, Arslan CA, Tehrani MS, Khorami M, Hasanipanah M (2019) Simulating the peak particle velocity in rock blasting projects using a neuro-fuzzy inference system. Eng Comput 35(4):1203–1211
54. Hasanipanah M, Bakhshandeh Amnieh H, Arab H, Zamzam MS (2018) Feasibility of PSO–ANFIS model to estimate rock fragmentation produced by mine blasting. Neural Comput Appl 30(4):1015–1024
55. Zhou J, Li C, Arslan CA, Hasanipanah M, Amnieh HB (2019) Performance evaluation of hybrid FFA-ANFIS and GA-ANFIS models to predict particle size distribution of a muck-pile after blasting. Eng Comput. https://doi.org/10.1007/s00366-019-00822-0
56. Hasanipanah M, Zhang W, Armaghani DJ, Rad HN (2020) The potential application of a new intelligent based approach in predicting the tensile strength of rock. IEEE Access 8:57148–57157
57. Nikafshan Rad H, Jalali Z, Jalalifar H (2015) Prediction of rock mass rating system based on continuous functions using Chaos–ANFIS model. Int J Rock Mech Min Sci 73:1–9
58. Shahnazar A, Nikafshan Rad H, Hasanipanah M, Tahir MM, Armaghani DJ, Ghoroqi M (2017) A new developed approach for the prediction of ground vibration using a hybrid PSO-optimized ANFIS-based model. Environ Earth Sci 76(15):527
59. Salimi H (2015) Stochastic fractal search: a powerful metaheuristic algorithm. Knowl Based Syst 75(2015):1–18
60. Mosbah H, El-Hawary ME (2017) Optimization of neural network parameters by Stochastic Fractal Search for dynamic state estimation under communication failure. Electr Power Syst Res 147:288–301
61. Rezakazemi M, Dashti A, Asghari M, Shirazian S (2017) H2-selective mixed matrix membranes modeling using ANFIS, PSO-ANFIS, GA-ANFIS. Int J Hydrog Energy 42:15211–15225
62. Hasanipanah M, Armaghani DJ, Amnieh HB, Majid MZA, Tahir MMD (2017) Application of PSO to develop a powerful equation

for prediction of flyrock due to blasting. Neural Comput Appl 28(1):1043–1050
63. Hajihassani M, Armaghani DJ, Kalatehjari R (2018) Applications of particle swarm optimization in geotechnical engineering: a comprehensive review. Geotech Geol Eng 36(2):705–722
64. Luo Z, Hasanipanah M, Amnieh HB, Brindhadevi K, Tahir MM (2019) GA-SVR: a novel hybrid data-driven model to simulate vertical load capacity of driven piles. Eng Comput. https://doi.org/10.1007/s00366-019-00858-2
65. Chen W, Hasanipanah M, Rad HN, Armaghani DJ, Tahir MM (2019) A new design of evolutionary hybrid optimization of SVR model in predicting the blast-induced ground vibration. Eng Comput. https://doi.org/10.1007/s00366-019-00895-x
66. Hasanipanah M et al (2018) Prediction of an environmental issue of mine blasting: an imperialistic competitive algorithm-based fuzzy system. Int J Environ Sci Technol 15(3):551–560
67. Jahed Armaghani D, Hasanipanah M, Mahdiyar A, Abd Majid MZ, Bakhshandeh Amnieh H, Tahir MMD (2018) Airblast prediction through a hybrid genetic algorithm-ANN model. Neural Comput Appl 29(9):619–629
68. Yang HQ et al (2018) Effects of joints on the cutting behavior of disc cutter running on the jointed rock mass. Tunn Undergr Space Technol 81:112–120
69. Nikafshan Rad H, Bakhshayeshi I, Wan Jusoh WA, Tahir MM, Kok Foong L (2019) Prediction of flyrock in mine blasting: a new computational intelligence approach. Nat Resour Res. https://doi.org/10.1007/s11053-019-09464-x
70. Lu X, Hasanipanah M, Brindhadevi K, Amnieh HB, Khalafi S (2019) ORELM: a novel machine learning approach for prediction of flyrock in mine blasting. Nat Resour Res. https://doi.org/10.1007/s11053-019-09532-2
71. Zhao YR, Yang HQ et al (2019) Mechanical behavior of intact completely decomposed granite soils along multi-stage loading–unloading path. Eng Geol 260:105242. https://doi.org/10.1016/j.enggeo.2019.105242
72. Sun G, Hasanipanah M, Amnieh HB, Foong LK (2020) Feasibility of indirect measurement of bearing capacity of driven piles based on a computational intelligence technique. Measurement 156:107577
73. Amiri M, Hasanipanah M, Amnieh HB (2019) Predicting ground vibration induced by rock blasting using a novel hybrid of neural network and itemset mining. Neural Comput Appl. https://doi.org/10.1007/s00521-020-04822-w
74. Fang Q, Nguyen H, Bui XN, Nguyen-Thoi T (2019) Prediction of blast-induced ground vibration in open-pit mines using a new technique based on imperialist competitive algorithm and M5Rules. Nat Resour Res. https://doi.org/10.1007/s11053-019-09577-3
75. Yang H, Liu F, Lin S (2020) Investigation on the 3D ground settlement induced by shallow tunneling considering the effects of buildings. KSCE J Civ Eng 24:365–376. https://doi.org/10.1007/s12205-020-2201-9
76. Jahed Armaghani D et al (2020) Examining hybrid and single SVM models with different kernels to predict rock brittleness. Sustainability 12(6):2229
77. Liu B, Yang H, Karekal S (2020) Effect of water content on argillization of mudstone during the tunnelling process. Rock Mech Rock Eng 53:799–813. https://doi.org/10.1007/s00603-019-01947-w
78. Jing H, Rad HN, Hasanipanah M, Armaghani DJ, Qasem SN (2020) Design and implementation of a new tuned hybrid intelligent model to predict the uniaxial compressive strength of the rock using SFS-ANFIS. Eng Comput. https://doi.org/10.1007/s00366-020-00977-1
79. Hasanipanah M, Amnieh HB (2020) A fuzzy rule-based approach to address uncertainty in risk assessment and prediction of blast-induced Flyrock in a quarry. Nat Resour Res 29(2):669–689
80. Harandizadeh H, Armaghani DJ, Mohamad ET (2020) Development of fuzzy-GMDH model optimized by GSA to predict rock tensile strength based on experimental datasets. Neural Comput Appl. https://doi.org/10.1007/s00521-020-04803-z
81. Yang Y, Zang O (1997) A hierarchical analysis for rock engineering using artificial neural networks. Rock Mech Rock Eng 30:207–222